Int. J. High Technology Ceramics 1 (1985) 107–118

Sintering and Strength of Silicon Nitride–Silicon Carbide Composites

Hidehiko Tanaka*, Peter Greil and Günter Petzow

Max-Planck Institut für Metallforschung, Institut für Werkstoffwissenschaften, Pulvermetallurgisches Laboratorium, Heisenbergstr. 5, D-7000 Stuttgart 80, FRG

SUMMARY

The sintering, microstructure, fracture toughness and strength of silicon carbide-dispersed silicon nitride composite systems were investigated. The composite powders could be sintered with aluminium oxide and yttrium oxide additives at normal pressure. Nearly complete densification was achieved by hipping presintered compacts. The silicon carbide particle dispersion retarded both grain and pore growth during sintering. The strength was found to increase with silicon carbide content, whereas fracture toughness remained constant. Thus strengthening of the composite is attributed to the decrease in flaw size.

1. INTRODUCTION

Silicon nitride and silicon carbide materials exhibit excellent high temperature mechanical properties and are candidates for application as structural materials in heat engines. Improvement of the mechanical properties of silicon nitride and silicon carbide-based materials has also focused on the dispersion of second-phase particles.[1–5] Dispersed zirconium dioxide or hafnium dioxide particles of up to 20 vol.% were found to increase the fracture toughness.[6,7] This was attributed to the stress-induced tetragonal to monoclinic phase transformation of zirconium dioxide or the formation of microcracks in the matrix. Lange,[1] and Wei and Becher[4] reported that the fracture toughness can also be increased by silicon

* Present address: National Institute of Research in Inorganic Materials, Sakura-mura, Ibaraki-ken, Japan.

Int. J. High Technology Ceramics 0267-3762/85/$03·30

carbide particle dispersion in a silicon nitride matrix and likewise by titanium carbide particles in silicon carbide. Usually, the particle-dispersed silicon nitride or silicon carbide matrix materials were prepared by hot-pressing, because the second phase did not promote densification. Common sintering additives able to sinter both matrix and second-phase particles were seldom found.

Fine silicon nitride powder can be sintered easily by the addition of aluminium oxide and yttrium oxide,[8] resulting in microstructures with glassy or crystalline grain boundary phases, respectively. Omori and Takei[9] found that the combination of aluminium oxide and yttrium oxide can also be used to sinter silicon carbide powder under normal pressure. The densification process in both systems is supposed to be dominated by a liquid-phase sintering mechanism, where the liquid is formed by the oxide additives and the silicon dioxide impurity content of the powders. Thus the Al_2O_3–Y_2O_3 oxide system seems to be a possible sintering additive for a silicon carbide-dispersed silicon nitride matrix material, i.e. silicon nitride–silicon carbide composite.

In this work the pressureless sintering of silicon nitride–silicon carbide composites with the additives aluminium oxide and yttrium oxide was investigated. Hot isostatic pressing (hipping) was applied to provide further densification. The effects of silicon carbide dispersion on the microstructure formation and the mechanical properties of the composite were studied.

2. EXPERIMENTAL

Pure and fine grain α-Si_3N_4 powder (H. C. Starck, LC 10) and β-SiC powder (H. C. Starck, B 10) were used as the starting materials. These modifications are both low temperature forms. The mean grain sizes of the silicon nitride and silicon carbide powders were 0·5 and 1·0 μm, respectively. The powders containing fixed amounts of silicon nitride and silicon carbide were mixed with aluminium oxide (Alcoa, A 16) and yttrium oxide (Ventron, 4 N) powders by the attritor mill, and cold isostatically pressed at 630 MPa.

These powder compacts were subsequently sintered in a graphite element furnace under 0·1 MPa nitrogen. The bend strength and the fracture toughness were measured at room temperature. Inner and outer spans for 4-point bend tests were 20 and 40 mm, respectively. The indentation strength-in-bending technique (ISB)[10] was used for measuring fracture toughness. Indentation forces were 29·4–196·2 N and the span of the 3-point bend test for ISB was 12 mm.

The microstructure of the specimens was observed by scanning electron microscopy (SEM) on the polished and etched surfaces. Molten sodium

hydroxide and Murakami's reagent were used as the etching materials. The molten sodium hydroxide etched the oxynitride grain boundary phase and the Murakami's reagent etched the silicon carbide grains. From the photomicrographs the areas of pores and grains which appeared on the polished and etched surfaces were counted and measured.

Hipping was performed with nitrogen at 100 MPa and 2000 °C. The samples were presintered at 1850 °C and were not encapsulated. The strength and fracture toughness of the hipped samples were also measured.

3. RESULTS AND DISCUSSION

3.1. Sintering

Figure 1 shows the density of sintered silicon nitride as a function of the total amount of oxide additives and the content of aluminium oxide in the additive. From the results given in Fig. 1, it was decided that the amount of oxide additive for the pressureless sintering of silicon nitride–silicon carbide composite materials should be 15 wt % and the weight content of aluminium oxide in the additive, $Al_2O_3/(Al_2O_3 + Y_2O_3)$, was chosen as 0·7.

Figure 2 shows the relationship between the weight fraction of silicon carbide and the relative density of the composites which were sintered in the temperature range 1600–1850 °C. The sinterability of the silicon nitride–silicon carbide composite powder was found to be lower than that of

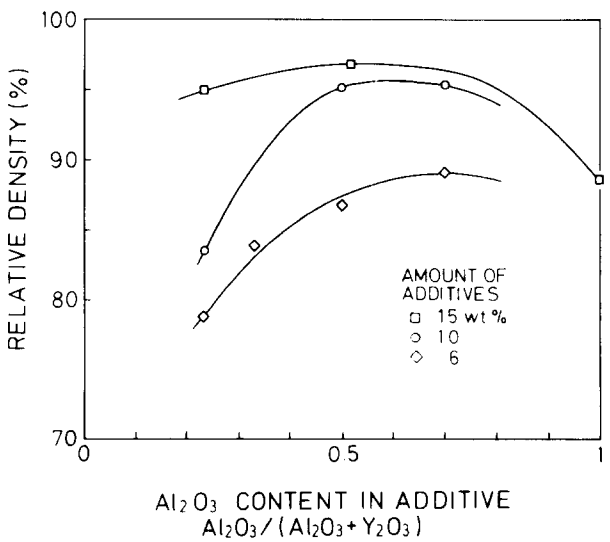

Fig. 1. Sintering density of silicon nitride powder with yttrium oxide and aluminium oxide additions. The sintering was carried out at 1800 °C for 30 min.

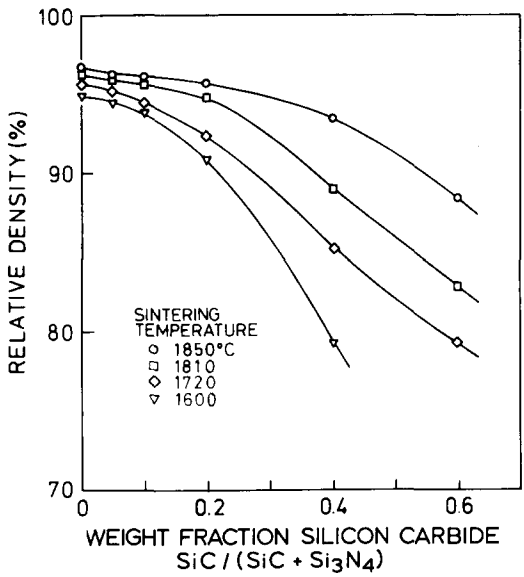

Fig. 2. Density of silicon nitride–silicon carbide composites as a function of the weight fraction [SiC/(SiC + Si_3N_4)] of silicon carbide content. Samples were sintered with 10·5 wt % aluminium oxide and 4·5 wt % yttrium oxide in the temperature range 1600–1850 °C for 1 h.

pure silicon nitride, but it was possible to sinter it to nearly the same density as silicon nitride if the composite contained less than 20 wt % silicon carbide and it was sintered at 1850 °C. The powder X-ray diffraction measurement detected only β-Si_3N_4 and β-SiC phases in the sintered samples. Silicon nitride transformed completely from α- to β-phase, but the silicon carbide remained β-SiC.

Figure 3 shows the microstructure of the sintered composites. The optical micrographs reveal the β-SiC grains in bright contrast lying in the dark silicon nitride matrix. Figure 4 shows a SEM micrograph of the surface etched by Murakami's reagent. The silicon carbide grains exhibit rough surfaces and are very well dispersed in the continuous silicon nitride matrix. The bonding between silicon carbide and silicon nitride seems to be strong. It is suggested that the oxide melt wetted both silicon carbide and silicon nitride grains during sintering.

3.2. Strength and microstructure

Table 1 lists the results of strength and fracture toughness measurements of the composites. All samples were sintered with 10·5 wt % aluminium oxide and 4·5 wt % yttrium oxide at 1850 °C. The strength was found to increase with the silicon carbide dispersion up to a silicon carbide fraction of 0·1. The fracture toughness, however, did not exhibit any increase with silicon

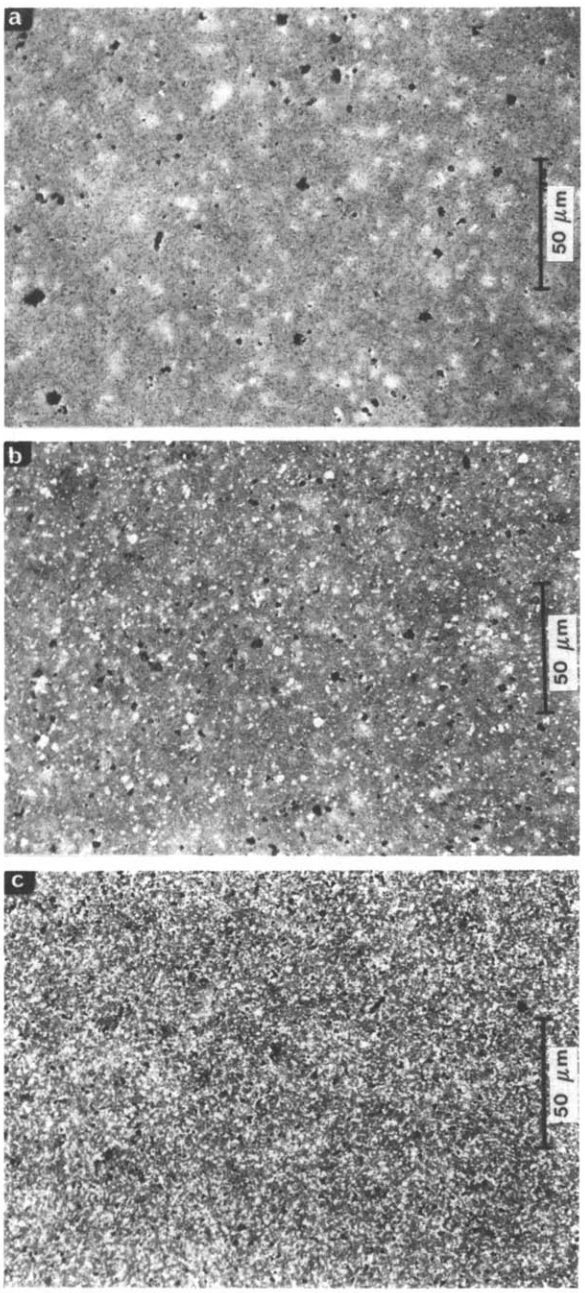

Fig. 3. Optical micrographs of polished surfaces. Weight fraction silicon carbide contents are (a) 0, (b) 0·2 and (c) 0·4. (Additive composition 10·5 wt % aluminium oxide and 4·5 wt % yttrium oxide; sintering conditions 1850 °C for 1 h.)

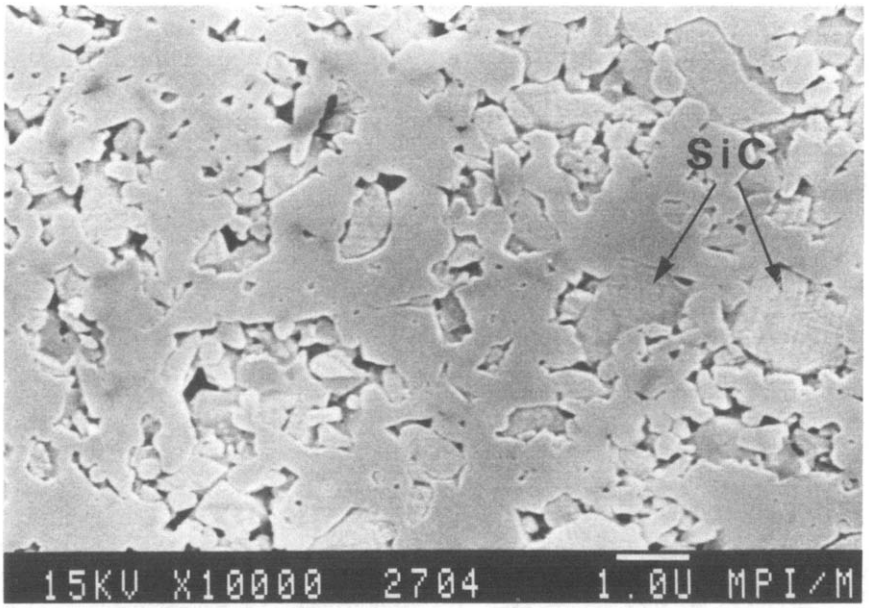

Fig. 4. SEM photograph showing silicon carbide grains in a silicon nitride matrix. The composite contains a silicon carbide weight fraction of 0·4 and was etched by Murakami's reagent. (Additives and sintering conditions as for Fig. 3.)

TABLE 1
Strength and K_{Ic} of Normal Sintered Composites

Sample		σ/*MPa*	K_{Ic}/$MN\,m^{-1.5}$	c/μm
$SiC/(SiC+Si_3N_4)$	ρ/% *theoretical*			
0	96·0	348 ± 108	3·95 ± 0·13	100
0·05	95·3	405 ± 28		
0·1	94·9	439 ± 31	3·94 ± 0·11	63
0·2	92·0	273 ± 56		
0·4	91·7	208 ± 57	3·17 ± 0·15	180
0·6	87·0	291 ± 78		

$SiC/(SiC+Si_3N_4)$ = content of SiC.
ρ = relative density at 20 °C.
σ = mean 20 °C 4-point bend strength.
K_{Ic} = mean 20 °C fracture toughness by ISB method.
c = expected flaw size calculated from σ and K_{Ic}.

carbide dispersion. Samples containing a silicon carbide fraction of 0·2 or more show lower strength and fracture toughness, which can be attributed to the increasing residual porosity after sintering.

Concerning the mechanical properties of the particle-dispersed ceramic, there are many mechanisms which are supposed to strengthen the matrix materials. Internal stresses due to thermal expansion or elasticity mismatch affect the strength. The proposed mechanisms are the prestressing of the dispersed phase,[11] the deflection of the propagating crack by a stress field[4,12] and energy dissipation by microcracking.[13–15] The dispersed particles can also act as obstacles to the crack propagation. The effects of crack pinning[16] and the crack deflection by inclusions have been reported to be effective in ceramic composite systems.[1,17]

All the mechanisms mentioned above mainly increase the fracture toughness, K_{Ic}, of the composite material as compared to the pure matrix material.[18] The strengthening effect is therefore mainly attributed to the increase of the fracture toughness if the critical flaw size remains unchanged by particle dispersion.

In this work an increase of fracture strength with silicon carbide dispersion was found, but the fracture toughness remained fairly constant. The toughening mechanism did not appear. Thus the increase of fracture strength may be explained by the decrease of the critical flaw size due to dispersed silicon carbide particles. Table 1 summarizes the results of an estimation of the critical flaw size, c, which was calculated from the fracture strength, σ_B, and fracture toughness, K_{Ic}, by using the Griffith equation $c = (K_{Ic}/Y\sigma_B)^{1/2}$, with Y equal to 1·13 when a penny-shaped crack is assumed. The smallest flaw size at fracture was estimated to be about 60 μm in the specimen containing a silicon carbide fraction of 0·1.

Figure 5 shows the microstructures of the samples containing a silicon carbide fraction of 0 and 0·2. The silicon carbide-containing microstructure clearly reveals a smaller grain size and a better homogeneity as compared to the silicon carbide-free sintered silicon nitride; this is also confirmed by the optical micrographs of the polished surfaces given in Fig. 3. The results of quantitative microstructure analysis are given in Fig. 6. The mean areas of pores and grains are plotted against the weight fraction of silicon carbide in the composite in a semi-logarithmic scale. The mean pore and grain sizes decrease with increasing weight fraction of silicon carbide. It follows that the dispersion of silicon carbide particles in the silicon nitride matrix retarded both pore and grain growth during sintering. The mean pore and grain diameters of $\sim$ 1–2 μm and even their maximum values (7 μm for the grains and 12 μm for the pores) do not correspond to the estimated critical flaw size.

Thus the silicon carbide dispersion seems to result in a shift of the pore and grain size distributions to smaller sizes after pressureless sintering with a

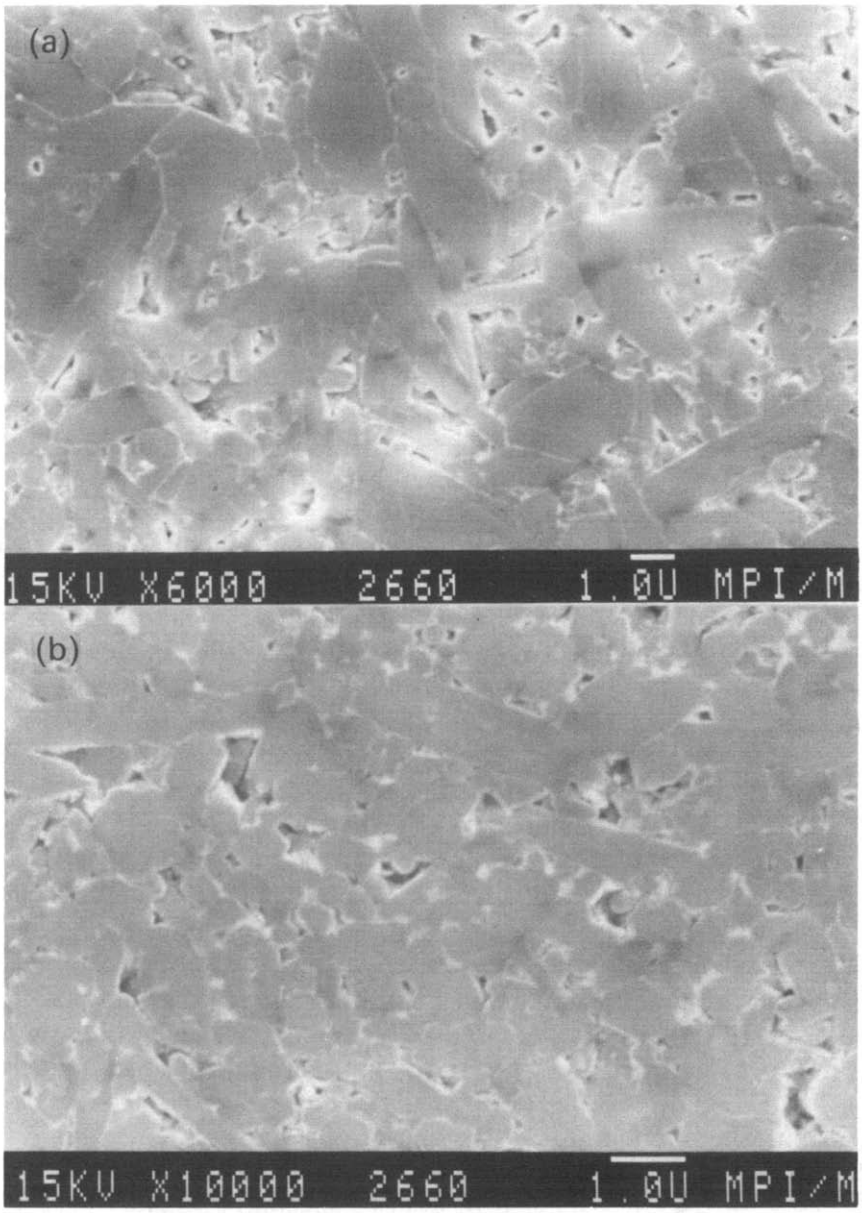

Fig. 5. Microstructure of (a) silicon carbide-free sintered silicon nitride; (b) composite containing a silicon carbide fraction of 0·2.

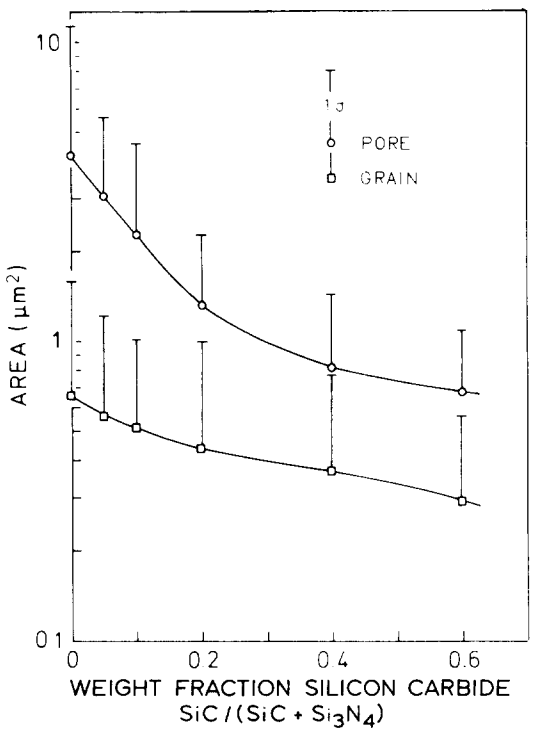

Fig. 6. Mean pore and grain areas as a function of weight fraction of silicon carbide content in the composite. The mean values were obtained by the counting of 100–280 pores and 230–300 grains on the SEM photographs.

more homogeneous microstructure as compared to the silicon carbide dispersion-free silicon nitride material.

3.3. Strength of composite after hipping

The results of the strength measurements suggest that the decrease in fracture strength in silicon carbide-rich composites is mainly attributed to residual porosity after pressureless sintering. Hipping was applied so that complete densification could also be attained in composites containing a silicon carbide fraction of $> 0{\cdot}2$. The results of the hipping treatment are given in Fig. 7 and Table 2. After hipping, the densities were calculated to be $\sim 97\%$ of theoretical density in the samples with a silicon carbide fraction of 0–0·4, and 96% in the sample with a fraction of 0·6.

Pressure-assisted densification of silicon nitride ceramics during hipping was reported to be strongly time-dependent.[19] In this investigation, hipping for 10 min and 50 min at 2000 °C resulted in almost the same densities. Thus 10-min hipping seemed to be sufficient for densification even though a small amount (2–3%) of residual porosity still remained.

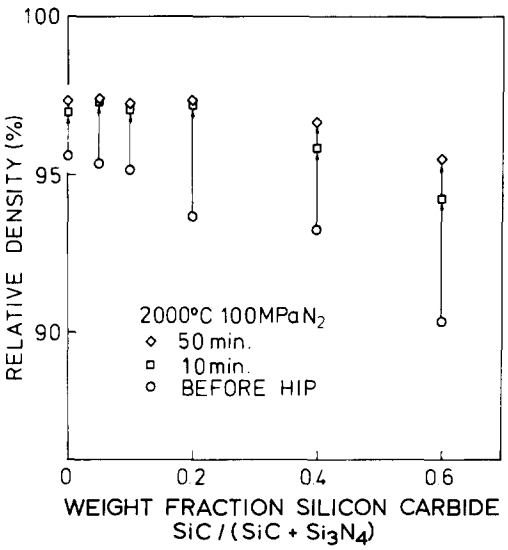

Fig. 7. Increase in relative density after hipping at 2000 °C and 100 MPa nitrogen pressure for 10 min and 50 min.

The mechanical properties of the hipped samples are listed in Table 2. A distinct improvement of fracture strength occurred, whereas fracture toughness was slightly degraded by silicon carbide dispersion. A mean fracture stress of 561 MPa was determined in the specimen containing a silicon carbide fraction of 0·4 with a fracture toughness of only 3·3 MN $m^{-3/2}$. The results show that the main effect of hipping is to decrease the flaw size in the composite system. The small pore size and good homogeneity of the presintered silicon carbide–silicon nitride composite

TABLE 2
Strength and K_{Ic} after Hipping

Sample		σ/*MPa*	K_{Ic}/*MN* $m^{-1.5}$	c/μ*m*
$SiC/(SiC+Si_3N_4)$	ρ/% *theoretical*			
0	96·9	352 ± 33	3·85 ± 0·20	95
0·1	96·6	491 ± 101	3·55 ± 0·35	41
0·4	96·6	561 ± 38	3·30 ± 0·08	27

$SiC/(SiC+Si_3N_4)$ = content of SiC.
ρ = relative density at 20 °C.
σ = mean 20 °C 4-point bend strength.
K_{Ic} = mean 20 °C fracture toughness by ISB method.
c = expected flaw size calculated from σ and K_{Ic}.

microstructure seem to be particularly suitable for the application of hipping to silicon nitride-based materials.

4. CONCLUSIONS

The sintering and mechanical properties of silicon carbide dispersed in a silicon nitride matrix composite were investigated. The mixture of α-Si_3N_4 and β-SiC fine powders could be sintered at normal pressure with aluminium oxide and yttrium oxide additives. The composites with silicon carbide fractions of 0·05 and 0·1 had higher strength than the sintered silicon nitride. Silicon carbide dispersion retarded both grain and pore growth, but did not toughen the composite materials. Thus strengthening is explained by a reduction of the critical flaw size. The hipping process was effective in further densifying the presintered silicon carbide-containing composites. Strengths improved after hipping and increased with silicon carbide content. Further hipping markedly decreased the flaw size in the composite system.

REFERENCES

1. Lange, F. F., Effect of microstructure on the strength of Si_3N_4–SiC composite system, *J. Am. Ceram. Soc.*, **56** (1973) 445.
2. Mah, T., Mendiratta, M. G. and Lipsitt, H. A., Fracture toughness and strength of Si_3N_4–TiC composites, *Am. Ceram. Soc. Bull.*, **60** (1981) 1229.
3. Faber, K. T. and Evans, A. G., Intergranular crack deflection toughening in silicon carbide, *J. Am. Ceram. Soc.*, **66** (1983) C94.
4. Wei, G. C. and Becher, P. F., Improvements in mechanical properties in SiC by addition of TiC particles, *J. Am. Ceram. Soc.*, **67** (1984) 571.
5. Greskovich, C. and Palm, J. A., Observations on fracture toughness of β-Si_3N_4–β-SiC composites, *J. Am. Ceram. Soc.*, **63** (1980) 597.
6. Claussen, N. and Jahn, J., Mechanical properties of sintered and hot-pressed Si_3N_4–ZrO_2 composites, *J. Am. Ceram. Soc.*, **61** (1978) 94.
7. Gauckler, L. J., Lorenz, J., Weiss, J. and Petzow, G., Improved fracture toughness of SiC-based ceramics, *Sci. Ceram.*, **10** (1980) 577.
8. Smith, J. and Quackenbush, C. L., A study of sintered Si_3N_4 compositions with Y_2O_3 and Al_2O_3 densification additives, in *Proc. Int. Symp. Factors in Densification and Sintering of Oxide and Non-oxide Ceramics*, Eds S. Sōmiya and S. Saito, KTK Publ. Tokyo, 1978, 426.
9. Omori, M. and Takei, H., Pressureless sintering of SiC, *J. Am. Ceram. Soc.*, **65** (1982) C92.
10. Anstis, G. R., Chantikul, P., Lawn, B. R. and Marshall, D. B., A critical evaluation of indentation techniques for measuring fracture toughness. I, direct crack measurements, *J. Am. Ceram. Soc.*, **64** (1981) 533.
11. Evans, A. G., The role of inclusions in the fracture of ceramic materials, *J. Mat. Sci.*, **9** (1974) 1145.

12. Nadeau, J. S. and Dickson, J. I., Effect of internal stress due to a dispersed phase on the fracture toughness of glass, *J. Am. Ceram. Soc.*, **63** (1980) 517.
13. Davidge, R. W. and Green, T. J., The strength of two phase ceramic/glass materials, *J. Mat. Sci.*, **3** (1968) 629.
14. Kreher, W. and Pompe, W., Increased fracture toughness of ceramics by energy dispersive mechanisms, *J. Mat. Sci.*, **16** (1981) 694.
15. Evans, A. G. and Faber, K. T., Toughening of ceramics by circumferential microcracking, *J. Am. Ceram. Soc.*, **64** (1981) 394.
16. Lange, F. F., The interaction of a crack front with a second phase, *Phil. Mag.*, **22** (1970) 983.
17. Faber, K. T. and Evans, A. G., Crack deflection processes, *Acta Met.*, **31** (1983) 565.
18. Rice, R. W., Mechanisms of toughening in ceramic matrix composites, *Ceramic Engineering and Science Proc.*, **2** (1981) 661.
19. Hirota, H., Ichikizaki, T. and Yajima, Y., Hot isostatic pressing of normally sintered silicon nitride in nitrogen gas as pressure medium, *Yogo-Kyokai-Shi*, **92** (1984) 188.

Received 16 September 1985; accepted 28 October 1985